

# Combustion behaviour and emission trends of diesel–jp8 blends in a single-cylinder diesel engine

Fazıl Akgün<sup>1</sup> , Samet Çelebi<sup>2,3\*</sup> , Usame Demir<sup>4</sup> 

<sup>1</sup>Bilecik Seyh Edebali University, Vocational School, Department of Motor Vehicles Transportation Technologies, Bilecik, Türkiye

<sup>2</sup>Sakarya University of Applied Sciences, Arifiye Vocational School, Department of Motor Vehicles Transportation Technologies, Sakarya, Türkiye

<sup>3</sup>Sakarya University of Applied Sciences, Automotive Technologies Application and Research Center, Sakarya, Türkiye

<sup>4</sup>Bilecik Seyh Edebali University, Faculty of Engineering, Department of Mechanical Engineering, Bilecik, Türkiye

**Abstract:** This study investigates the effects of blending JP8 fuel with conventional diesel on engine performance, combustion characteristics, and exhaust emissions in a single-cylinder, four-stroke, direct-injection diesel engine. Tests were conducted at 1800 rpm under five torque loads (0, 8, 16, 24, and 32 Nm) using three fuel types: pure diesel, 90% diesel–10% JP8 (90D10JP8), and 70% diesel–30% JP8 (70D30JP8). Results showed that at low loads (8 Nm), JP8 blends exhibited higher BSFC values (e.g., 404.1 g/kWh for 70D30JP8 vs. 376.4 g/kWh for diesel) and lower BTE (20.54% vs. 21.89%), consistent with prior findings on JP8's lower cetane number and volatility. However, at full load (32 Nm), both JP8 blends achieved better BSFC (249.19 g/kWh for 70D30JP8 vs. 277.96 g/kWh for diesel) and higher BTE (33.31% vs. 29.64%), indicating improved combustion under high thermal loads—a trend also observed in studies on kerosene-based blends enhancing atomization at elevated temperatures. Combustion analysis revealed that JP8 blends delayed ignition (e.g., CA10 at -2.29°CA for 70D30JP8 vs. -3.20°CA for diesel) and prolonged combustion duration at mid-loads (26.68 CAD for 70D30JP8 at 16 Nm vs. 23.93 CAD for diesel), in line with literature describing increased premixed fractions due to lower cetane number. Despite this, maximum in-cylinder pressure surpassed diesel at 16 Nm (76.88 bar for 70D30JP8 vs. 72.76 bar for diesel), indicating stronger premixed combustion. Emission results confirmed CO reductions at full load for JP8 blends (0.402% vs. 0.834% for diesel) and notable soot suppression at mid-loads (e.g., at 24 Nm: 0.46% for 70D30JP8 vs. 8.57% for diesel), consistent with JP8's lower aromatic content. However, NO<sub>x</sub> emissions increased at mid-to-high loads (e.g., at 32 Nm: 999 ppm for 70D30JP8 vs. 930 ppm for diesel), highlighting a trade-off due to higher local combustion temperatures. Overall, this study expands existing knowledge by providing a detailed, load-dependent evaluation of JP8–diesel blends, showing that blends—particularly at 30% JP8 can achieve comparable or superior performance at high loads while reducing CO and soot emissions, although NO<sub>x</sub> mitigation strategies remain essential for practical application.

**Keywords:** JP8, diesel engine, performance, emissions, combustion

## 1. Introduction

Jet Propellant 8 (JP8) is a multi-purpose military aviation fuel that has emerged as a critical component in modern defense logistics due to its adaptability, availability, and performance characteristics [1]. Originally developed to replace the more volatile JP-4, JP8 has become the standard fuel for NATO forces and is extensively used by the United States military in aircraft, ground vehicles, and even heating systems. [2–4] Its formulation emphasizes safety [5], thermal stability, and multi-platform applicability, positioning it as a strategic

energy resource with growing interest in civilian sectors as well[6]. JP8 is produced through the refinement of crude oil, but its adaptability allows it to be synthesized from alternative feedstocks, including natural gas via gas-to-liquid (GTL) technologies, biomass through Fischer-Tropsch processes, and even from waste plastics or coal-based liquefaction routes[7]. This diversity in sourcing not only provides logistical security during military operations but also aligns with global efforts to develop more resilient fuel supply chains[8,9]. Its chemical structure consists mainly of kerosene-range hydrocarbons, paraffins, naphthenes, and aromatics, which

\*Corresponding author:

Email: scelebi@subu.edu.tr

Cite this article as:

Akgün, F., Çelebi, A., Demir U. (2025). Combustion behaviour and emission trends of diesel–jp8 blends in a single-cylinder diesel engine. *European Mechanical Science*, 9(3): 263-276. <https://doi.org/10.26701/ems.1697763>

History dates:

Received: 13.05.2025, Revision Request: 21.06.2025, Last Revision Received: 30.06.2025, Accepted: 03.08.2025



© Author(s) 2025. This work is distributed under <https://creativecommons.org/licenses/by/4.0/>

offer balanced combustion and volatility characteristics [10,11]. Typical properties include a density of approximately 775–840 kg/m<sup>3</sup>, a cetane number in the range of 40–45, and a lower heating value (LHV) of ~43 MJ/kg. These parameters make it suitable for compression ignition engines, albeit with performance trade-offs compared to standard diesel fuel [12]. The effects of JP8 on diesel engine performance and emissions are due to differences in the physical and chemical properties of the fuel [13]. In general, there may be minor losses in torque and fuel economy when JP8 is used in a diesel engine, but there is potential for reduced particulate matter (PM) and NO<sub>x</sub> emissions [14]. Due to the lower density and viscosity of JP8, torque and fuel economy may be reduced compared to a diesel engine. However, these losses can be compensated for by increasing the injection duration and similar performance to diesel fuel can be achieved [15]. The lower cetane number of JP8 increases ignition delay and causes more premixed combustion. This changes the combustion characteristics of the engine [16,17]. Blends of JP8 and biodiesel can be used without a significant loss of engine performance. When using the optimum blend ratios, engine efficiency and performance can be maintained [18]. Use of JP8 reduces NO<sub>x</sub> and particulate matter emissions under most conditions, especially when used in conjunction with exhaust gas recirculation (EGR) and multiple injection strategies [19,20]. JP8 tends to reduce smoke and CO emissions, but under some conditions, increased HC (hydrocarbon) and CO emissions may be observed [21–24]. In JP8 and biodiesel blends, NO<sub>x</sub> emissions increase while CO emissions decrease. Smoke and total hydrocarbon emissions vary depending on the blend ratio [14]. From an environmental standpoint, JP8 shows potential benefits. Previous studies have demonstrated its ability to reduce particulate matter (PM) and smoke emissions, largely due to its lower aromatic content and higher hydrogen-to-carbon ratio compared to diesel. The application of JP8 in diesel engines has been associated with reductions in soot, CO, and unburned hydrocarbons under certain conditions, especially when optimized through engine calibration strategies such as advanced injection timing or the use of exhaust gas recirculation (EGR). Fernandes et al. (2007) observed significant reductions in soot formation when JP8 was used in a heavy-duty diesel engine, although NO<sub>x</sub> emissions required additional control measures such as selective catalytic reduction (SCR) [25]. Despite these advantages, using JP8 in conventional diesel engines poses some challenges. Its lower viscosity and density may result in suboptimal fuel injection patterns, especially in mechanical injection systems, leading to decreased atomization and air–fuel mixing [26]. Additionally, prolonged exposure to JP8 may affect lubricity-sensitive components in the fuel system, such as injector tips and pump seals, necessitating either fuel system redesign or the addition of lubricity-enhancing additives [27]. Another factor influencing the combustion behavior of JP8 is its complex distillation range and evaporation characteristics. These attributes can affect cold start performance and transient

response, particularly under low ambient temperatures. For this reason, JP8 is not commonly used as a direct replacement in civilian vehicles without engine modification or calibration. However, its use in blended form—particularly with diesel or biodiesel—has emerged as a practical strategy to combine the benefits of both fuels. Such blends allow leveraging JP8's volatility and cleaner combustion potential while maintaining the favorable ignition properties and energy density of diesel. Numerous experimental studies have investigated the effects of JP8–diesel blends on engine behavior. Uyumaz et al. (2014) conducted combustion and emission measurements in a single-cylinder direct injection diesel engine using JP8–biodiesel blends and reported a trade-off between NO<sub>x</sub> and soot emissions [28]. Tsanaktisidis et al. (2014) explored ternary blends involving JP8, diesel, and biodiesel and emphasized improvements in storage stability and volatility profiles. These studies generally confirm that moderate ratios of JP8 (e.g., 10–30%) can be successfully incorporated into diesel fuel without significant degradation in engine performance, provided appropriate control strategies are applied [29]. A notable feature of JP8–diesel blends is their impact on combustion phasing. The ignition delay caused by JP8 can alter the crank angle at which key combustion events—such as 10%, 50%, and 90% cumulative heat release—occur. These shifts influence both the efficiency and emissions of the engine. For instance, a delay in CA50 (crank angle at 50% heat release) may reduce thermal efficiency, while a wider combustion duration (from CA10 to CA90) could enhance soot oxidation under high-temperature conditions. Understanding these dynamics is essential for calibrating engines to exploit the full potential of JP8-based fuels [14]. Beyond conventional energy-based assessments, exergy and second-law analyses offer deeper insights into the thermodynamic performance of fuel-blend combustion systems. Recent studies have demonstrated the value of exergy-based optimization in integrated energy systems [30–35], suggesting that similar approaches could be applied to evaluate diesel–JP8 blends, optimize combustion strategies, and minimize irreversibilities.

Moreover, the suitability of JP8–diesel blends under varying engine load conditions remains an area of ongoing research. Most studies have focused on either full-load or low-load steady-state operations, with limited data available for intermediate load ranges where modern engines often operate. Mid-load conditions are particularly relevant for optimizing fuel consumption and emissions in real-world driving cycles. Under such regimes, the volatility and combustion reactivity of JP8 become more influential, possibly offering improved premixed combustion behavior and enhanced heat release characteristics. In the context of modern emission regulations and alternative fuel strategies, JP8–diesel blends present both a challenge and an opportunity. On one hand, their usage requires careful attention to fuel system compatibility, combustion optimization, and after-treatment integration. On the other, they offer a pathway to fuel standardization across military and ci-

vilian fleets, reduced dependency on petroleum-based diesel, and alignment with net-zero emission goals when derived from renewable feedstocks.

Despite its promising attributes, the literature lacks a comprehensive and systematic evaluation of JP8–diesel blends under multi-load conditions in a controlled laboratory environment. Specifically, there is a scarcity of experimental studies detailing how JP8 influences in-cylinder pressure development, heat release rate (HRR) behavior, combustion phasing (e.g., CA10, CA50, CA90), and cumulative heat release trends across various loads. Moreover, there is limited clarity on how these combustion dynamics translate into real-world engine performance metrics such as brake thermal efficiency (BTE), brake specific fuel consumption (BSFC), and regulated emissions ( $\text{NO}_x$ , CO, HC, soot,  $\text{CO}_2$ ). Therefore, the main purpose of this study is to experimentally investigate the feasibility of using JP8–diesel blends as alternative fuels in compression ignition engines by evaluating their effects on combustion behavior, performance characteristics, and emission profiles under various engine loads. The experimental work is conducted using a single-cylinder, four-stroke, air-cooled diesel engine operating at a constant speed of 1800 rpm under five distinct torque loads (0, 8, 16, 24, and 32 Nm). By comparing two JP8–diesel blend ratios (10% and 30%) with pure diesel, this study aims to bridge the aforementioned knowledge gap and provide practical insights into the optimization of alternative fuel strategies for both military and civilian engine platforms.

## 2. Materials and Methods

The experimental work was conducted in the Engine Test and Simulation Laboratory of Sakarya University of Applied Sciences, Arifiye Vocational School. The engine used for the tests was a single-cylinder, four-stroke, air-cooled, direct-injection diesel engine, model Antor 3LD510. ►Table 1 provides detailed technical specifications of the engine.

**Table 1.** Technical specifications of the test engine

Properties	Value/Description
Model	Antor 3LD510
Cylinder Number	1
Cooling Type	Air Cooling
Bore × Stroke	85 × 90 (mm × mm)
Total Cylinder Volume	510 ( $\text{cm}^3$ )
Maximum Power	12.0 HP (9.0 kW) @ 3000 RPM
Maximum Torque	32.8 Nm @1800 RPM
Compression Ratio	17.5:1
Maximum Speed	3000 RPM

In this study, all tests were performed at a constant engine speed of 1800 rpm, corresponding to the speed at which the engine generates its maximum torque. Engine loads were applied at five discrete torque values: 0 Nm, 8 Nm, 16 Nm, 24 Nm, and 32 Nm. The engine was first operated using conventional diesel fuel to obtain baseline data. Subsequently, two fuel blends—90% diesel + 10% JP8 (90D10JP8) and 70% diesel + 30% JP8 (70D30JP8) were tested under identical operating conditions. Three fuels were injected via the main direct-injection system. All performance and emission measurements reported represent averages from at least two repeated trials at each operating condition to ensure repeatability. Standard deviations were calculated and will be included as error bars in all revised plots.

A 15 kW DC electric dynamometer (KEMSAN brand) was used for applying engine load. Torque measurements were obtained using an “S-type” load cell integrated with the dynamometer system. Fuel consumption was quantified by recording the mass of fuel consumed over a 60-second interval using a high-precision balance and a stopwatch. Each measurement point was repeated at least twice to ensure repeatability and reliability.

In-cylinder pressure data were collected using an AVL GH14P piezoelectric pressure sensor installed on the engine cylinder head. The pressure signals were amplified through an AVL charge amplifier and transferred to the AVL Indi-Com combustion analysis system. Crank angle information was measured with an AVL crank encoder and synchronized with pressure data for combustion analysis. The pressure data were filtered using a fourth-order digital filter to remove high-frequency noise and improve signal quality.

Exhaust gas temperature was monitored with a K-type thermocouple mounted on the exhaust manifold. Emissions of CO,  $\text{CO}_2$ , HC,  $\text{NO}_x$ , and  $\text{O}_2$  were analysed using a BILSA MOD 2210 WINXP-K gas analyser. The measurement range and precision of this device are listed in ►Table 2.

**Table 2.** Technical Specifications of Emission Measuring Device

Parameter	Measurement Limit	Sensitivity
CO	0 - 10%	0.01%
$\text{CO}_2$	0 - 20%	0.01%
HC	0 - 10000 ppm	1 ppm
$\text{O}_2$	0 - 25%	0.01%
$\text{NO}_x$	0 - 5000 ppm	1 ppm
Lambda	0 - 5	0.001

Throughout the experiments, injection timing and fuel quantity were kept constant, with only fuel type varied. Engine speed was continuously monitored with a

tachometer linked to the dynamometer system. Dynamometer load and engine throttle position were controlled via an integrated panel. The overall experimental setup is shown schematically in ►Figure 1.

The key physical and chemical properties of JP8 fuel compared to conventional diesel are summarized in ►Table 3. These differences play a significant role in fuel behavior, combustion dynamics, and emission characteristics. JP8 exhibits a lower density (approximately 775–840 kg/m<sup>3</sup>) than diesel (820–860 kg/m<sup>3</sup>), which can influence fuel injection quantity and combustion energy output. Additionally, JP8 has a significantly lower viscosity (1.25–1.90 mm<sup>2</sup>/s at 40°C) compared to diesel (1.9–4.1 mm<sup>2</sup>/s), which facilitates better atomization and vaporization but may pose long-term durability concerns for fuel system components due to reduced lubricity. JP8 also has a lower cetane number (typically 40–45) than diesel (45–55), which contributes to longer ignition delay and a greater premixed combustion phase. This altered combustion phasing may result in higher pressure rise rates and increased formation of NO<sub>x</sub> and HC emissions under certain conditions. Despite this, the lower aromatic content of JP8 (<25% compared to <35% in diesel) promotes cleaner combustion and contributes to reduced soot formation, particularly under medium-load operation. Furthermore, JP8's flash point is approximately ≥38°C, which is lower than that of diesel (≥55°C), making it more volatile and easier to ignite, although it requires careful handling in storage and transport. Interestingly, both fuels offer

comparable lower heating values, with JP8 around 43.2 MJ/kg and diesel ranging from 42.5 to 43.0 MJ/kg, suggesting that JP8 can deliver similar energy content per unit mass when properly combusted. These properties collectively affect engine calibration, combustion efficiency, and emission profiles, which are thoroughly evaluated in the present study under different load conditions.

**Table 3.** Physical and chemical properties of Jet Propellant 8 (JP8) fuel

Property	JP8 Fuel	Diesel Fuel
Density @15°C (kg/m <sup>3</sup> )	~775–840	~820–860
Viscosity @40°C (mm <sup>2</sup> /s)	1.25–1.90	1.9–4.1
Cetane Number	40–45	45–55
Lower Heating Value	~43.2	~42.5–43.0
Flash Point (°C)	≥ 38	≥ 55
Aromatic Content (%)	< 25	< 35

## 2.1. Uncertainty Analysis

To ensure the reliability and validity of the experimental results, an uncertainty analysis was conducted for the measured key parameters including torque, fuel consumption, in-cylinder pressure, and exhaust emissions. Both systematic and random uncertainties were taken into account, and the total uncertainty for each measurement was estimated using the root sum square

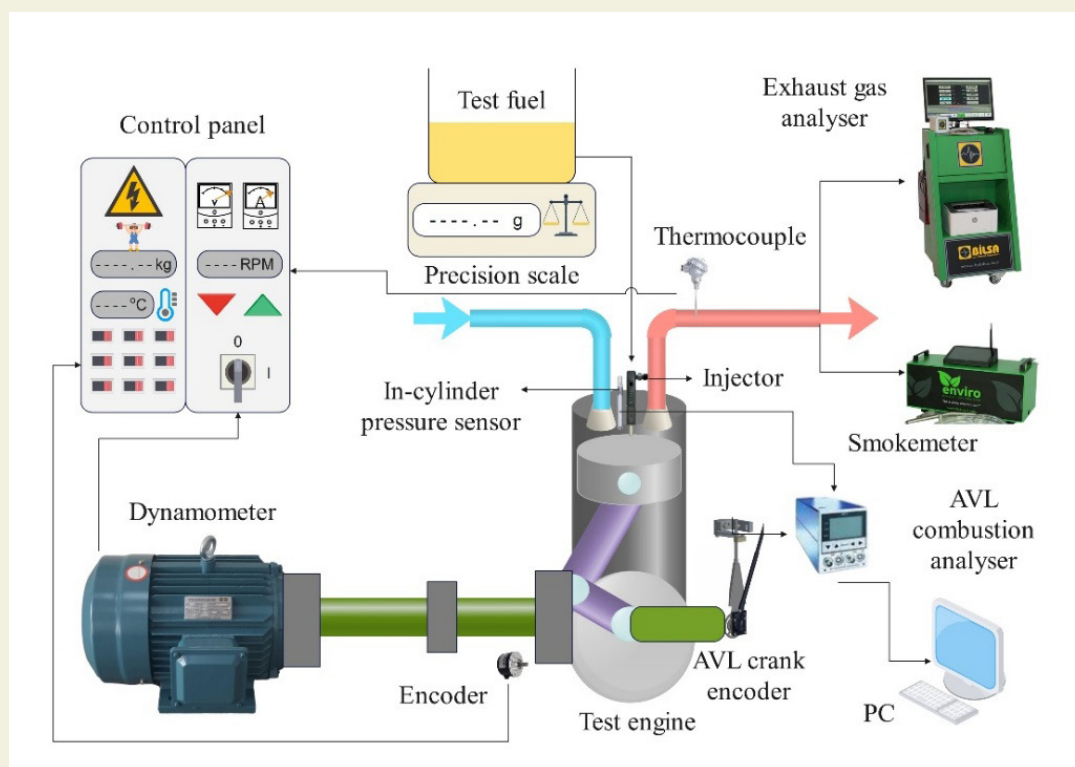


**Figure 1.** Experimental test setup

(RSS) method as specified in the Kline and McClintock approach.

The measurement uncertainty of the torque measurements obtained from the S-type load cell integrated into the dynamometer system is  $\pm 0.1$  Nm. Fuel consumption was measured gravimetrically over a 60-second interval using a high-precision balance with a resolution of 0.01 g, and the overall uncertainty in the fuel mass flow rate was estimated as  $\pm 0.5\%$ .

The in-cylinder pressure was measured using an AVL GH14P piezoelectric pressure sensor with a sensitivity of 0.1 pC/bar and an accuracy of  $\pm 1\%$ , and data acquisition was synchronized with the crank angle via a high-resolution AVL crank encoder. Although the signal was digitally filtered to reduce noise, a residual uncertainty of  $\pm 1.5\%$  was taken into account in the pressure measurements.

For exhaust emissions, a BILSA MOD 2210 WINXP-K gas analyzer was used with instrument-specific accuracies listed in ►Table 2. Based on the manufacturer's calibration specifications and repeatability trials, the measurement uncertainties were  $\pm 0.01\%$  for CO and CO<sub>2</sub>,  $\pm 1$  ppm for NO<sub>x</sub> and HC, and  $\pm 0.01\%$  for O<sub>2</sub>.

The combined uncertainties for derived performance parameters, such as Brake Thermal Efficiency (BTE) and Brake Specific Fuel Consumption (BSFC), were propagated using standard error propagation formulas that accounted for both torque and fuel mass flow uncertainties. The estimated uncertainty in BTE was  $\pm 1.2\%$ , while the uncertainty in BSFC was  $\pm 1.5\%$ .

To increase repeatability, all experimental points were repeated at least twice, and the standard deviations of the repeated measurements were within acceptable limits ( $<3\%$ ).

This methodological framework was applied to evaluate the impact of JP8–diesel fuel blends on engine performance, combustion behaviour, fuel consumption, and emission characteristics under varying load conditions.

### 3. Results and Discussions

In this section, the performance, combustion, and emission characteristics of pure diesel and JP8–diesel fuel blends (90D10JP8 and 70D30JP8) were comparatively evaluated under different engine load conditions. The experimental results were analysed in terms of brake thermal efficiency, fuel consumption, combustion phasing, in-cylinder pressure parameters, and pollutant emissions to assess the feasibility of using JP8 as a diesel substitute in compression ignition engines.

#### 3.1. Engine Performance Indicators

►Figure 2 presents the variation of brake specific fuel

consumption (BSFC) under different engine load conditions for pure diesel, 90D10JP8, and 70D30JP8 blends. BSFC shows an inverse relationship with load across all fuels, decreasing as load increases due to improved combustion efficiency and reduced frictional losses. At 8 Nm, BSFC was highest: 376.4 g/kWh for diesel, 401.0 g/kWh for 90D10JP8, and 404.1 g/kWh for 70D30JP8, reflecting incomplete combustion and higher heat losses, especially for JP8 blends with lower cetane number. At 16 Nm, BSFC dropped notably, with diesel at 268.2 g/kWh, 70D30JP8 at 288.8 g/kWh, and 90D10JP8 at 299.4 g/kWh, indicating slightly reduced fuel economy with higher JP8 content. At high loads (24 Nm and 32 Nm), JP8 blends achieved BSFC values comparable to or better than diesel. Notably, at 32 Nm, BSFC was 277.96 g/kWh for diesel, 252.76 g/kWh for 90D10JP8, and 249.19 g/kWh for 70D30JP8. This improvement is attributed to enhanced air–fuel mixing, combustion stability, and better atomization at higher temperatures, suggesting JP8 blends can offer competitive fuel economy under high-load conditions. [36].

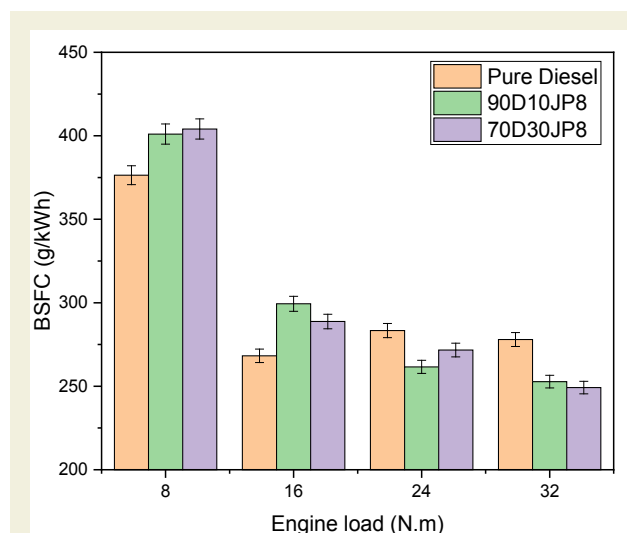


Figure 2. Variation of BSFC with engine load for different fuel types

►Figure 3 illustrates the variation of brake thermal efficiency (BTE) with engine load for pure diesel, 90D10JP8, and 70D30JP8 blends. BTE increased with load for all fuels due to improved combustion stability, higher in-cylinder temperatures, and reduced heat losses. At 8 Nm, BTE was lowest, with diesel at 21.89%, and slightly lower values for 90D10JP8 (20.59%) and 70D30JP8 (20.54%), reflecting their lower cetane number and energy content. At 16 Nm, diesel showed the highest BTE at 30.71%, while JP8 blends had mildly reduced efficiencies. However, at higher loads (24 Nm and 32 Nm), JP8 blends outperformed diesel. At 32 Nm, diesel achieved 29.64%, while 90D10JP8 and 70D30JP8 reached 32.67% and 33.31%, respectively. This improved high-load performance is attributed to better atomization and mixing of JP8 blends at elevated temperatures, suggesting their suitability for high-load diesel engine applications where thermal efficiency is critical. [36].

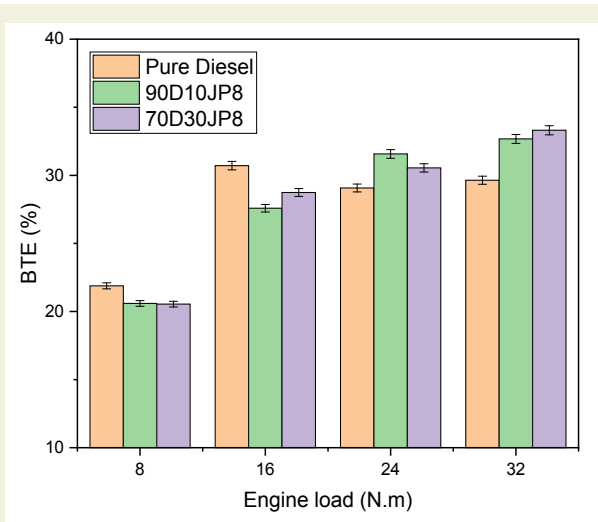


Figure 3. Variation of BTE with engine load for different fuel types.

### 3.2. Combustion Parameters

In ►Figure 4, the in-cylinder pressure, heat release rate and cumulative heat release values of the test fuels at 0, 8, 16, 24, and 32 Nm engine loads are shown graphically. As a general trend, it is seen that pure diesel fuel produces higher in-cylinder pressure values compared to JP8-added fuels as the load increases. This is thought to be due to the lower cetane number and lower energy content of JP8 compared to pure diesel. However, at 16 Nm load, JP8 blend produces higher maximum in-cylinder pressure compared to pure diesel, in addition to higher heat release rate and cumulative heat release values. These results show that JP8 blend provides performance improvement at medium engine load. At 16 Nm load, a significant increase is observed in  $P_{max}$ , MPRR and IMEP values with 10% and 30% JP8 blend. It is observed that it provides a significant decrease in HC

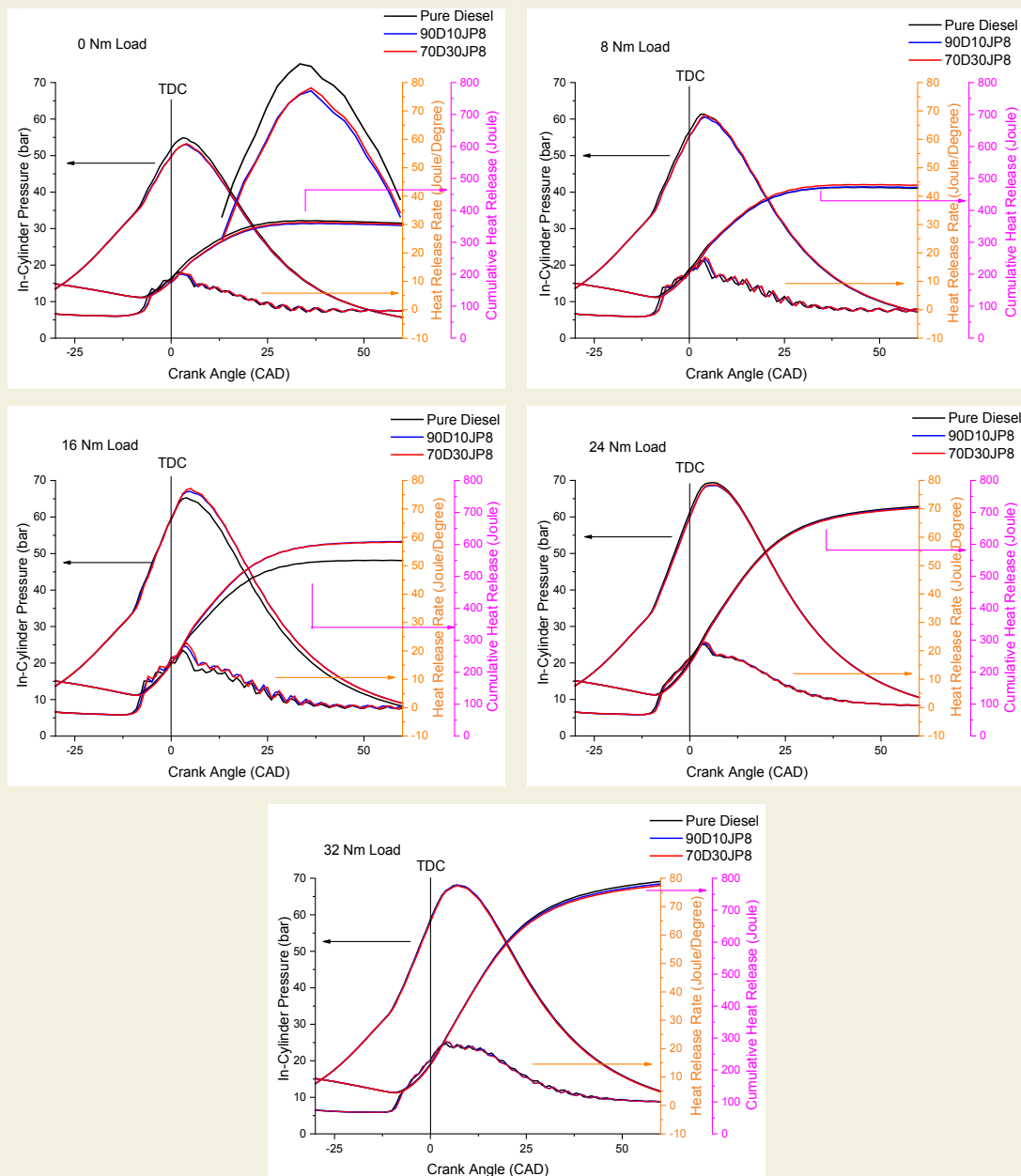


Figure 4. Changes in in-cylinder pressure, heat release and cumulative heat release of JP 8 blend at different loads

emissions. These results show that JP8 blend improves combustion at 16 Nm load. This improvement is probably due to improved fuel-air mixing and increased volatility of the JP8 mixture at moderate load conditions, which promotes more uniform combustion. The lower cetane number of JP8 slightly delayed ignition. An examination of the CA90 plot shows that combustion is delayed by the JP8 blend. The JP8 blend allows better premixing before combustion begins. This results in a rapid and intense combustion phase when ignition occurs, contributing to more complete combustion – hence the reduction in HC emissions. These effects are evident at 16 Nm load, indicating that JP8 exhibits favourable combustion kinetics under moderate in-cylinder pressure and temperature conditions.

► **Figure 5** displays the crank angle at 10% cumulative heat release (CA10), a key indicator of combustion start. CA10 marks the crank position where the first significant portion of fuel energy is released, helping evaluate ignition characteristics. Across all tested loads, JP8-containing blends (90D10JP8 and 70D30JP8) generally showed slightly advanced CA10 values compared to pure diesel. For instance, at 0 Nm, diesel ignited at  $-3.20^{\circ}\text{CA}$ , while 90D10JP8 and 70D30JP8 ignited at  $-2.52^{\circ}\text{CA}$  and  $-2.29^{\circ}\text{CA}$ , respectively. This behavior suggests that the lower cetane number and higher volatility of JP8 promote longer ignition delays, enabling better air-fuel premixing before ignition. As a result, combustion starts slightly earlier relative to TDC once ignition begins. This trend of advanced CA10 for JP8 blends remained consistent up to mid-loads. At 24 Nm, diesel showed  $-3.53^{\circ}\text{CA}$ , while the blends had slightly less advanced values of  $-3.14^{\circ}\text{CA}$  and  $-2.98^{\circ}\text{CA}$ , indicating the differences narrowed somewhat with load. At the highest load (32 Nm), CA10 values for all fuels converged closely (around  $-2.7^{\circ}\text{CA}$ ), suggesting that under high-pressure, high-temperature conditions, the influence of fuel type on ignition timing diminishes. These results highlight that while JP8 blends slightly modify combustion phasing at low and mid-loads, their effect becomes negligible at full load where in-cylinder conditions dominate ignition behavior. Across all operating conditions, CA10 values for JP8-containing blends (90D10JP8 and 70D30JP8) occurred earlier (i.e., closer to top dead center) than those of pure diesel fuel. This behavior is attributed to JP8's lower cetane number and higher volatility, which extend the ignition delay, allowing for more premixed combustion. As a result, once ignition begins, combustion proceeds rapidly. However, the shift in CA10 remains moderate, indicating that the blend ratios used do not dominate the ignition behavior entirely [37].

► **Figure 6** illustrates the crank angle at which 50% of the total heat release occurs (CA50), a key metric for combustion phasing and engine efficiency. Optimal CA50 values generally lie between  $5\text{--}10^{\circ}$  TDC to balance efficiency and knocking risk. At low engine loads (0 and 8 Nm), diesel exhibited earlier combustion phasing than the JP8 blends. For example, at 0 Nm,

diesel's CA50 was around  $-0.27^{\circ}\text{CA}$ , while 90D10JP8 and 70D30JP8 showed delayed phasing at  $1.06^{\circ}\text{CA}$  and  $1.43^{\circ}\text{CA}$ , respectively. This delay reflects the longer ignition delay of JP8-containing fuels due to their lower cetane number. As load increased to 16 Nm, CA50 values for all fuels moved closer to the optimal range. Diesel reached  $1.70^{\circ}\text{CA}$ , while JP8 blends recorded slightly later phasing at  $3.11^{\circ}\text{CA}$  and  $2.87^{\circ}\text{CA}$ . This moderate delay in the blends is consistent with their ignition characteristics but still acceptable for efficient operation. At higher loads (24 Nm and 32 Nm), differences between fuels narrowed further. For instance, at 24 Nm, diesel reached  $6.96^{\circ}\text{CA}$ , while JP8 blends were nearly identical at  $7.02^{\circ}\text{CA}$  and  $6.78^{\circ}\text{CA}$ . At full load (32 Nm), diesel peaked at  $10.17^{\circ}\text{CA}$ , with JP8 blends close behind around  $9.47^{\circ}\text{CA}$ . These results indicate that while JP8 blends cause slight delays in combustion phasing at low loads, their effect diminishes significantly as load

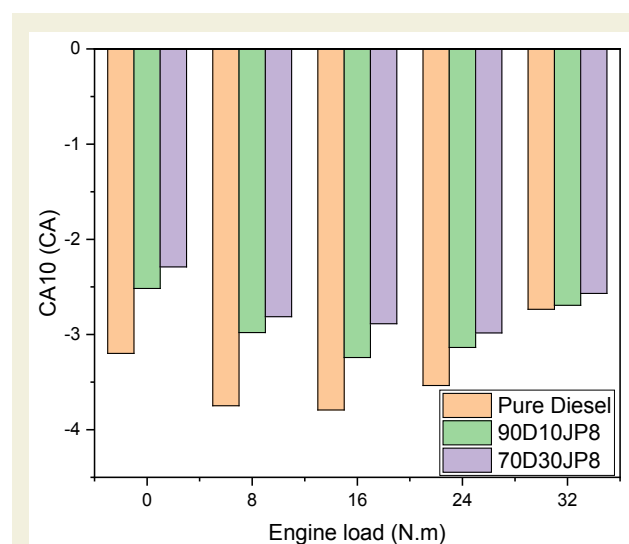


**Figure 5.** Variation of CA10 values with engine load for different fuel blends.

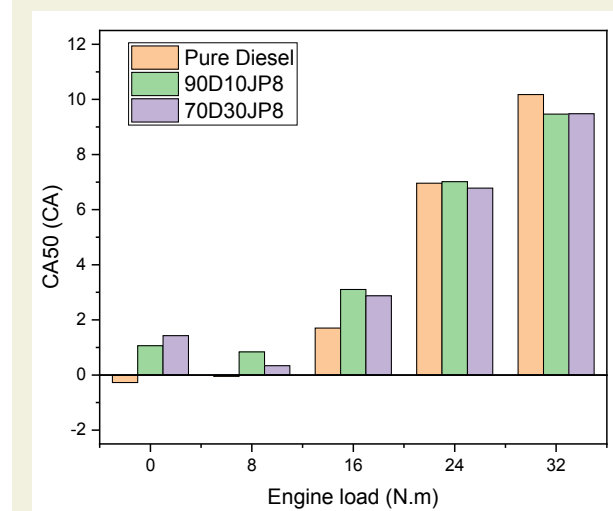


**Figure 6.** Variation of crank angle at 50% cumulative heat release (CA50) with engine load for different fuel types.

increases. At medium-to-high loads, all fuels achieve CA50 values within the ideal window, demonstrating that JP8–diesel blends can maintain efficient and stable combustion phasing suitable for practical diesel engine applications under higher load conditions.

► **Figure 7** presents the variation of CA90, representing the crank angle at which 90% of the fuel's heat is released—a key indicator of combustion duration and completeness. At low loads (0 Nm), diesel showed earlier combustion completion ( $12.56^\circ\text{CA}$ ) compared to JP8 blends ( $14.27^\circ\text{CA}$  and  $14.46^\circ\text{CA}$ ), indicating slightly longer combustion durations for the blends due to their lower cetane number and delayed ignition. As load increased to 16 Nm, this trend continued, with diesel at  $20.13^\circ\text{CA}$  and JP8 blends showing higher CA90 values of  $22.96^\circ\text{CA}$  and  $23.80^\circ\text{CA}$ , suggesting combustion extended further into the expansion stroke, potentially impacting thermal efficiency. However, at higher loads (24 and 32 Nm), differences between fuels narrowed significantly. At 24 Nm, CA90 values clustered around  $34\text{--}35^\circ\text{CA}$ , and at 32 Nm, diesel reached  $43.95^\circ\text{CA}$  while JP8 blends were only slightly lower ( $\sim 42.2\text{--}42.7^\circ\text{CA}$ ). This convergence at high loads is likely due to improved in-cylinder conditions that promote faster oxidation regardless of fuel blend. Overall, JP8 blends slightly prolong combustion at low and mid loads, but this effect becomes negligible at high loads, supporting their suitability for applications with variable load demands.

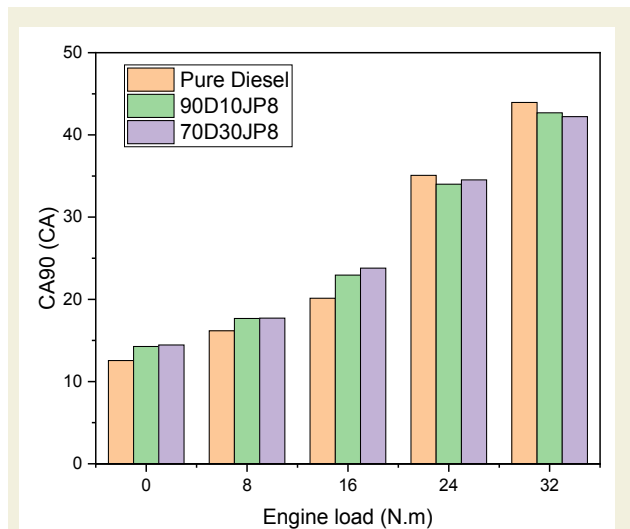


**Figure 7.** Variation of crank angle at 90% cumulative heat release (CA90) with engine load for different fuel types.

► **Figure 8** shows the variation of maximum in-cylinder pressure ( $P_{\max}$ ) across engine loads for diesel, 90D10JP8, and 70D30JP8 fuels.  $P_{\max}$  is a key indicator of combustion intensity and fuel reactivity. At idle (0 Nm), diesel recorded 59.47 bar, while JP8 blends were slightly lower ( $\sim 57.3$  bar), consistent with their delayed ignition and lower heat release. At 8 Nm,  $P_{\max}$  increased for all fuels, with values ranging from 68.01 bar (diesel) to 69.08 bar (70D30JP8). Notably, at 16 Nm, JP8 blends

surpassed diesel, with 70D30JP8 reaching 76.88 bar versus diesel's 72.76 bar, indicating enhanced premixed combustion from longer ignition delays. At 24 Nm, differences narrowed further, with all fuels around 73 bar, reflecting the dominant effect of in-cylinder conditions over fuel properties. At full load (32 Nm),  $P_{\max}$  values converged even more closely ( $\sim 72$  bar for all), suggesting minimal impact of blend ratio at high loads. Overall, while diesel maintained slightly lower pressures at mid-to-high loads, JP8 blends especially 70D30JP8 demonstrated comparable or higher peak pressures, highlighting their potential for efficient combustion under moderate and high loading conditions.

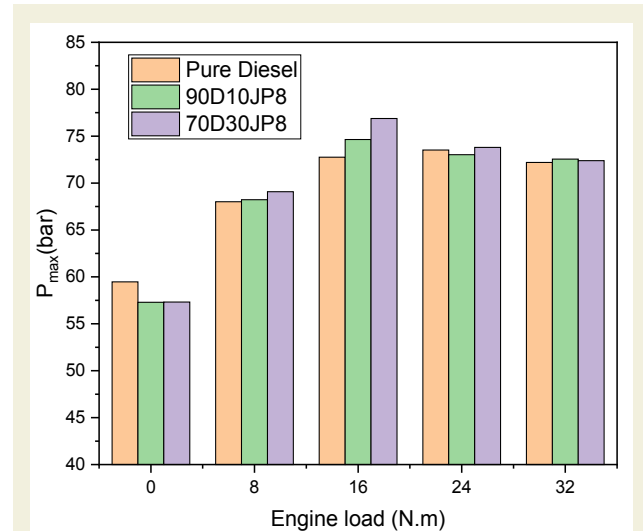
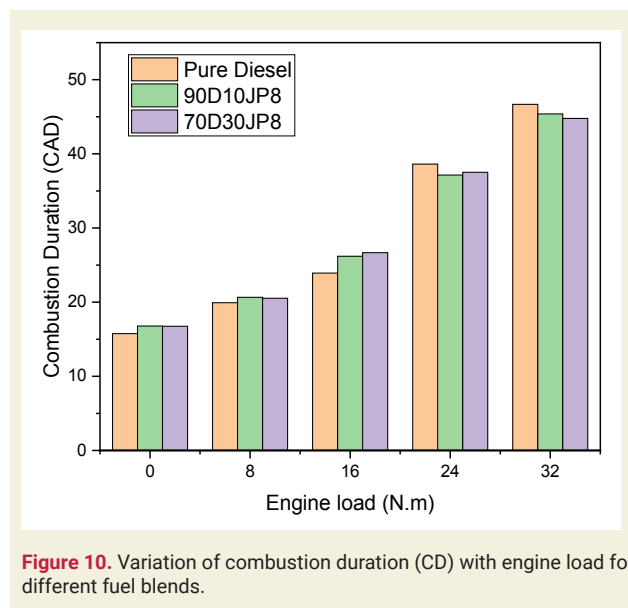
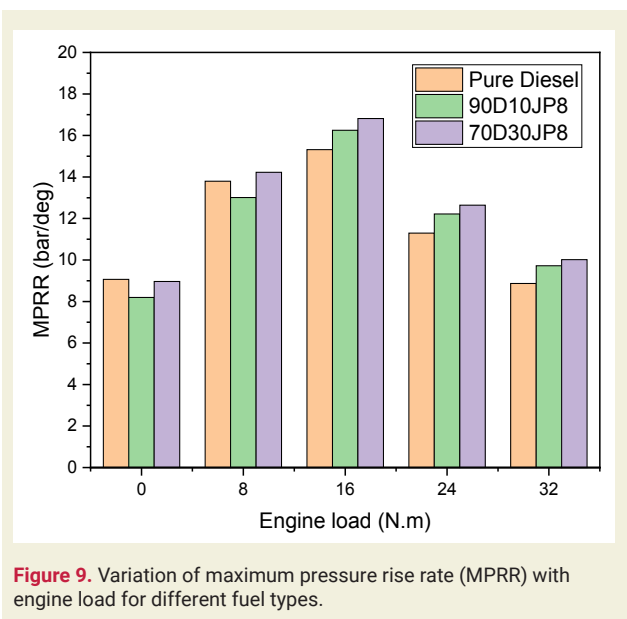


**Figure 8.** Variation of maximum in-cylinder pressure ( $P_{\max}$ ) with engine load for different fuel blends.

► **Figure 9** shows the variation of maximum pressure rise rate (MPRR) with engine load for diesel and JP8 blends. MPRR reflects how quickly in-cylinder pressure rises during combustion—a key indicator of premixed combustion intensity and potential knocking risk. At 0 Nm, MPRR values were moderate and similar across fuels: diesel at 9.07 bar/deg, with JP8 blends slightly lower (8.20–8.96 bar/deg), suggesting stable, low-load combustion. As load increased to 8 Nm, MPRR rose sharply, especially for JP8 blends. 70D30JP8 recorded 14.22 bar/deg versus 13.80 bar/deg for diesel, indicating stronger premixed combustion due to ignition delay. At 16 Nm, MPRR peaked for all fuels, with 70D30JP8 at 16.81 bar/deg, 90D10JP8 at 16.25 bar/deg, and diesel at 15.32 bar/deg. This reflects the most intense premixed combustion phase, particularly for higher JP8 ratios. Beyond 16 Nm, MPRR declined across all fuels as combustion shifted toward diffusion-controlled modes. At 32 Nm, values dropped to around 10 bar/deg, with diesel showing the lowest at 8.87 bar/deg. Overall, JP8 blends increase MPRR under mid-load conditions, enhancing combustion efficiency but also posing potential mechanical stress risks that should be considered in engine calibration.

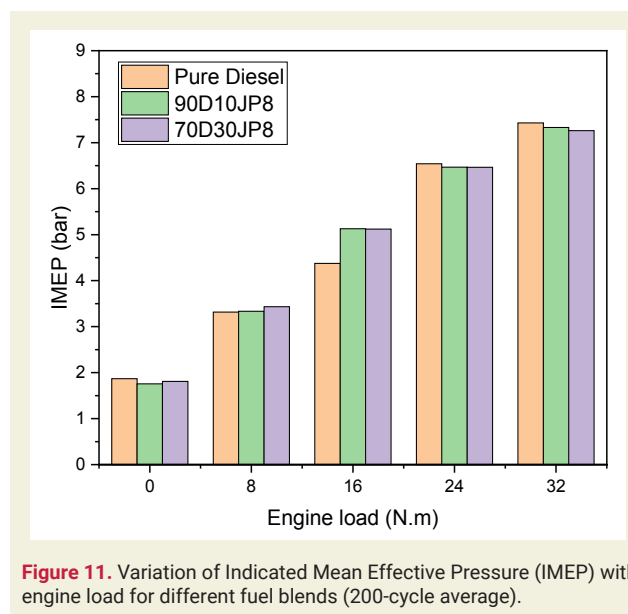
► **Figure 10** shows the effect of engine load on combustion



duration for diesel and JP8-diesel blends (90D10JP8 and 70D30JP8). Combustion duration, defined as the crank angle interval between CA10 and CA90, indicates how smoothly and efficiently combustion progresses. For all fuels, combustion duration increased with engine load. At low loads (0–8 Nm), durations were relatively short due to lower fuel mass and combustion intensity. At 0 Nm, diesel recorded 15.76 CAD, while JP8 blends were slightly longer (~16.8 CAD), reflecting delayed ignition and slower flame propagation from lower cetane number. At 16 Nm, differences became clearer: diesel reached 23.93 CAD, while JP8 blends extended to ~26–27 CAD, indicating a larger premixed combustion fraction and delayed phasing. At higher loads (24 and 32 Nm), combustion duration increased substantially for all fuels, but differences narrowed. For example, at 32 Nm, diesel reached 46.68 CAD, with JP8 blends close behind (~44.8–45.4 CAD), suggesting that elevated in-cylinder conditions mitigated delay effects. Overall, JP8 blends slightly increase combustion duration across loads due to delayed ignition, but this impact lessens at high loads where combustion conditions promote better fuel oxidation. These results align with trends observed in CA50, CA90, and MPRR analyses, highlighting greater sensitivity of JP8 combustion dynamics at low and mid-loads [38].

► **Figure 11** illustrates the variation of indicated mean effective pressure (IMEP) for diesel and JP8-diesel blends across engine loads. IMEP reflects the engine's ability to convert combustion energy into work, with values here averaged over 200 cycles for accuracy. At 0 Nm, IMEP was lowest for all fuels due to minimal fuel input: diesel at 1.869 bar, with JP8 blends slightly lower (~1.76–1.81 bar), showing little variation at idle. As load increased to 8 Nm, IMEP rose accordingly, with 70D30JP8 slightly exceeding diesel (3.43 bar vs. 3.32 bar), suggesting slightly stronger combustion. At 16 Nm, JP8 blends showed notably higher IMEP

(5.12–5.13 bar) than diesel (4.38 bar), consistent with stronger premixed combustion phases observed in  $P_{max}$  and MPRR trends. At higher loads (24 and 32 Nm), differences among fuels narrowed significantly. For example, at 32 Nm, diesel reached 7.43 bar, while JP8 blends were close behind (~7.26–7.33 bar), indicating reduced sensitivity to fuel type under high thermal conditions. Overall, these results confirm that JP8-diesel blends can deliver comparable or even slightly higher combustion effectiveness at low-to-mid loads, with performance differences becoming negligible at full load [37].



### 3.3. Emissions Trends

► **Figure 12** shows CO<sub>2</sub> emissions for diesel and JP8-diesel blends (90D10JP8 and 70D30JP8) across varying engine loads. As a primary product of complete combustion, CO<sub>2</sub> emissions generally rise with load due to increased fuel consumption. At 0 Nm, CO<sub>2</sub> levels were

low and similar: diesel and 70D30JP8 at 1.933%, and 90D10JP8 slightly lower at 1.787%, reflecting minimal combustion at idle. At 8 Nm, emissions rose modestly, with diesel at 3.42% and JP8 blends close behind (~3.30–3.46%), suggesting good combustion completeness. At 16 Nm, differences became clearer: diesel at 4.78%, while 90D10JP8 and 70D30JP8 were higher (5.41% and 5.22%), indicating better air–fuel mixing and more complete combustion from the JP8 blends. At higher loads (24 Nm and 32 Nm), CO<sub>2</sub> emissions peaked for all fuels, with values converging. For example, at 32 Nm, diesel reached 9.49%, while 90D10JP8 and 70D30JP8 were slightly lower (8.92–9.19%), suggesting that at full load, differences in blend composition have less impact than the dominant effect of high fuel delivery and combustion conditions. Overall, CO<sub>2</sub> emissions increased with load as expected. JP8 blends showed slightly higher emissions at mid-loads, reflecting efficient combustion, but differences narrowed at high loads where fuel quantity and load effects dominated [39,40].

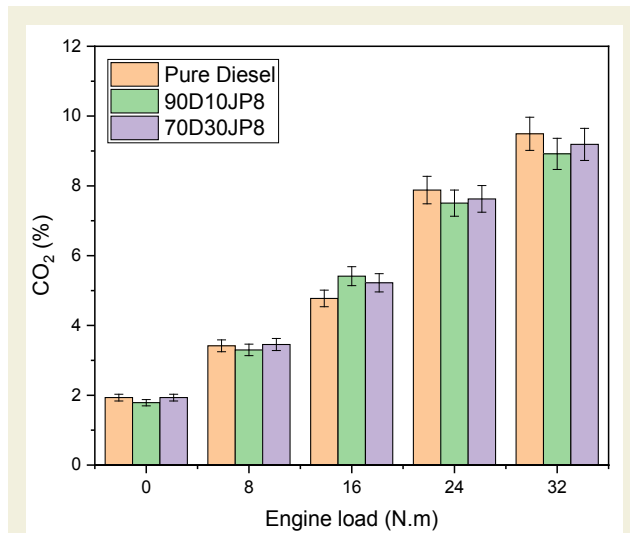


**Figure 12.** Variation of CO<sub>2</sub> emissions with engine load for different fuel blends.

► **Figure 13** shows CO emissions for diesel and JP8-diesel blends (90D10JP8 and 70D30JP8) across engine loads. CO forms from incomplete combustion, especially with rich mixtures or low combustion temperatures. At no-load (0 Nm), CO emissions were relatively high for all fuels due to poor combustion quality: diesel at 0.073%, with slightly higher values for JP8 blends (~0.076–0.079%), reflecting low temperatures and limited mixing. As load increased to 8 and 16 Nm, CO emissions dropped sharply for all fuels, indicating better combustion conditions and more complete oxidation to CO<sub>2</sub>. For example, at 16 Nm, diesel was at 0.020% and 70D30JP8 at 0.021%. At 24 Nm, CO emissions rose slightly, especially for diesel (0.099%), while JP8 blends remained lower (0.065–0.087%). This increase likely results from richer local zones at higher injection rates, where diesel's lower volatility limits mixing. At full load (32 Nm), the differences became more pronounced:

diesel emitted 0.834% CO, more than double the JP8 blends (around 0.40%). This suggests that JP8's better volatility and atomization promote more complete combustion even under demanding conditions. Overall, CO emissions were lowest at mid-loads and highest at idle and full load. JP8-diesel blends consistently showed lower CO at high loads, highlighting their advantage in improving combustion completeness under rich, high-demand conditions [41,42].

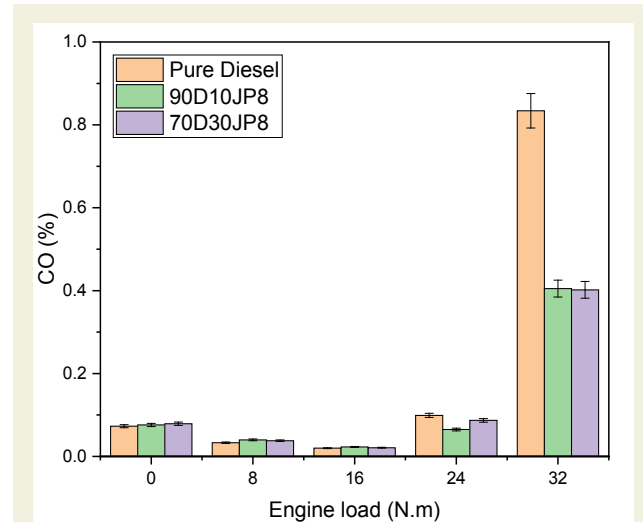


**Figure 13.** Variation of CO emissions with engine load for different fuel blends.

► **Figure 14** shows the change in unburned hydrocarbon (HC) emissions with engine load for diesel and JP8-diesel blends (90D10JP8 and 70D30JP8). HC emissions arise from incomplete combustion due to poor mixing, quenching near cold surfaces, or oxygen deficiency. At 0 Nm, HC emissions were low for all fuels: diesel at 18 ppm, with even lower values for JP8 blends (13–15 ppm), reflecting better volatility and atomization at idle. As load increased to 8 and 16 Nm, HC emissions rose moderately but remained lower for JP8 blends. At 16 Nm, diesel emitted 24 ppm, while JP8 blends were slightly lower (18–19 ppm), indicating improved pre-mixed combustion. At 24 Nm, diesel's HC spiked to 33 ppm, while JP8 blends stayed lower (~24–25 ppm), likely due to better mixing and combustion control. However, at full load (32 Nm), the trend reversed: diesel dropped to 16 ppm, while JP8 blends increased to ~28–29 ppm. This rise in HC for JP8 blends at high load may result from ignition delay, over-lean zones, or flame quenching under high-pressure conditions. Overall, JP8 blends reduce HC emissions at low and mid loads thanks to improved volatility and mixing, but may lead to higher HC at full load where combustion conditions become more demanding [43,44].

► **Figure 15** illustrates NO<sub>x</sub> emissions for diesel and JP8-diesel blends (90D10JP8 and 70D30JP8) across engine loads. NO<sub>x</sub> formation depends on combustion temperature and oxygen availability, typically increasing with load. At idle (0 Nm), NO<sub>x</sub> levels were low for

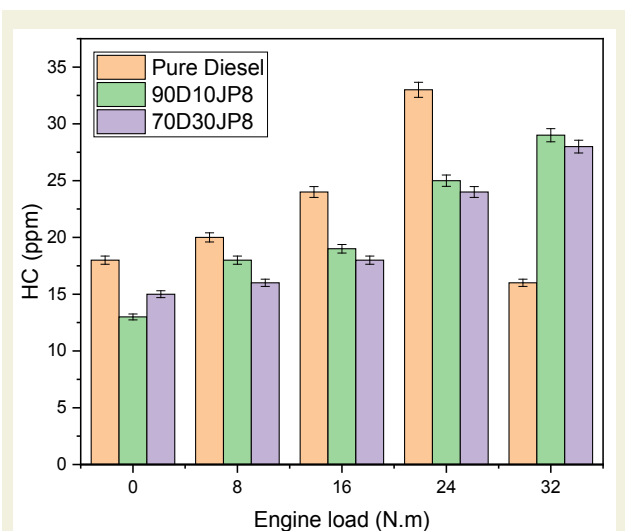


**Figure 14.** Variation of HC emissions with engine load for different fuel blends.

all fuels: diesel at 139 ppm, with JP8 blends even lower (100–114 ppm) due to cooler combustion and minimal injection. At 8 Nm, emissions rose sharply but remained lower for JP8 blends (405–427 ppm) compared to diesel (475 ppm), likely due to delayed ignition and slightly cooler peak temperatures. However, at 16 Nm, JP8 blends produced higher NO<sub>x</sub> than diesel (943 ppm for 90D10JP8, 885 ppm for 70D30JP8 vs. 813 ppm for diesel), reflecting more intense premixed combustion and higher local temperatures. This trend continued at 24 Nm, with all fuels peaking around 1086–1147 ppm. At 32 Nm, NO<sub>x</sub> slightly declined, but JP8 blends remained higher (999–1021 ppm) than diesel (930 ppm), likely due to richer zones limiting oxygen but still sustaining higher peak temperatures in the JP8 blends. Overall, while JP8 blends reduced NO<sub>x</sub> at low loads, they tended to exceed diesel at mid-to-high loads, suggesting the need for strategies like EGR or after-treatment to manage NO<sub>x</sub> emissions in practical applications [45].

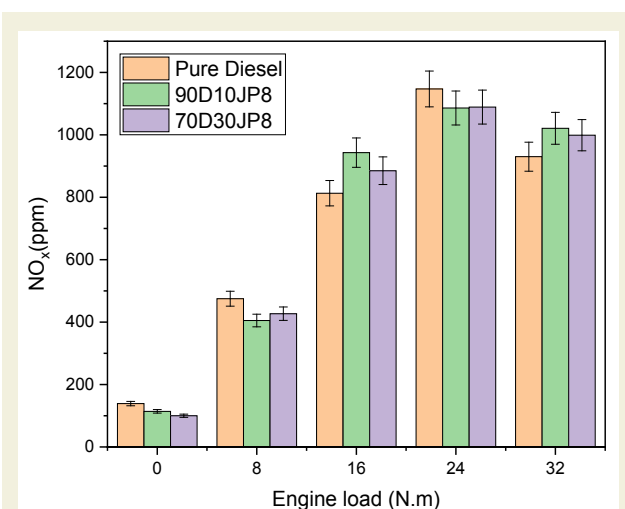


**Figure 15.** Variation of NO<sub>x</sub> emissions with engine load for different fuel blends.

► **Figure 16** illustrates soot emission levels for diesel and JP8-diesel blends (90D10JP8 and 70D30JP8) across engine loads. Soot forms under rich, low-oxygen conditions and is influenced by fuel composition and air–fuel mixing. At low loads (0–16 Nm), no detectable soot emissions were observed for any fuel, as lean, well-mixed combustion prevents soot formation. At 24 Nm, soot appeared, with diesel showing significantly higher emissions (8.57%) compared to much lower levels for 90D10JP8 (2.62%) and 70D30JP8 (0.46%). This reduction is attributed to JP8's lower aromatic content, higher hydrogen-to-carbon ratio, and better volatility, which promote cleaner combustion and more complete oxidation of soot precursors. However, at full load (32 Nm), soot emissions rose for all fuels. Diesel reached 14.41%, while 90D10JP8 and 70D30JP8 increased to 21.18% and 16.47%, respectively. Unlike at mid-loads, JP8 blends produced more soot than diesel, likely due to richer local zones and limited oxygen availability offsetting their volatility advantages. Overall, JP8-diesel blends effectively reduce soot at medium loads but may lead to higher emissions under high-load conditions where mixture richness and combustion complexity dominate [46].

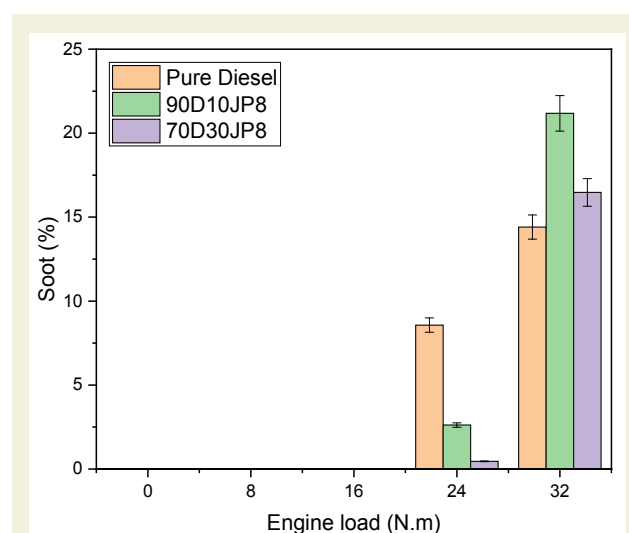


**Figure 16.** Variation of soot emissions with engine load for different fuel blends.

## 4. Conclusion

In this study, the effects of blending JP8 with conventional diesel fuel on engine performance, combustion behaviour, and exhaust emissions were experimentally investigated at different load conditions using a single-cylinder compression ignition engine. The main findings are summarized as follows:

- **Brake thermal efficiency (BTE)** increased with engine load for all fuels. At low load (8 Nm), JP8 blends showed about **6–7% lower BTE** than diesel (e.g., diesel at ~21.9% vs. ~20.5% for 70D30JP8), but at high load (32 Nm), **70D30JP8 exceeded diesel by ~12%** (33.31% vs. 29.64%), indicating su-

perior efficiency due to improved atomization and combustion.

- **Brake specific fuel consumption (BSFC)** was **~7–10% higher** for JP8 blends at low and mid loads (e.g., 404.1 g/kWh for 70D30JP8 vs. 376.4 g/kWh for diesel at 8 Nm), yet at full load (32 Nm), JP8 blends achieved **~10% lower BSFC** (e.g., 249.19 g/kWh for 70D30JP8 vs. 277.96 g/kWh for diesel), reflecting recovered combustion efficiency at elevated temperatures.
- **Combustion analysis** showed JP8 blends had delayed ignition (CA10 advanced by  $\sim 0.7$ – $1^\circ\text{CA}$ ), retarded combustion phasing (CA50  $\sim 1$ – $2^\circ\text{CA}$  later at mid loads), and **~10–12% longer combustion duration** (e.g.,  $\sim 26.7$  CAD vs.  $\sim 23.9$  CAD at 16 Nm). These differences diminished at high loads, where higher pressures improved ignition characteristics.
- **Peak in-cylinder pressure ( $P_{\max}$ ) and maximum pressure rise rate (MPRR)** were **~5–7% higher** for JP8 blends at mid loads (e.g.,  $P_{\max}$  of 76.88 bar for 70D30JP8 vs. 72.76 bar for diesel at 16 Nm), indicating more intense premixed combustion phases.
- **CO<sub>2</sub> emissions** increased with load for all fuels. At high load (32 Nm), JP8 blends showed **~3–6% lower CO<sub>2</sub>** than diesel (e.g., 8.92–9.19% vs. 9.49%), suggesting slightly leaner or more efficient combustion under maximum load.
- **CO and HC emissions** were generally **~10–30% lower** for JP8 blends at low and mid loads (e.g., CO at 16 Nm:  $\sim 0.02\%$  vs.  $\sim 0.021\%$  diesel), but increased at high load (32 Nm), where JP8 blends showed **~40–50% higher HC** than diesel (e.g.,  $\sim 28$ – $29$  ppm vs. 16 ppm).
- **NO<sub>x</sub> emissions** were **~15–30% lower** for JP8 blends at low load (e.g., 100 ppm vs. 139 ppm at idle), but exceeded diesel by **~5–15%** at mid and high loads (e.g., 999–1021 ppm vs. 930 ppm at 32 Nm), due to increased premixed combustion fractions and higher local temperatures.
- **Soot emissions** were drastically reduced with JP8 blends at mid loads, with reductions of **~80–95%** compared to diesel (e.g., at 24 Nm: 0.46% for 70D30JP8 vs. 8.57% for diesel), highlighting a major advantage in particulate emissions control.
- **Heat release rate (HRR) analysis** confirmed that JP8 blends delay and smooth combustion, producing **broader, lower peaks** while maintaining **comparable cumulative energy release**, supporting stable operation under varied loads.

In conclusion, JP8-diesel blends, especially with 30% JP8, show promise for diesel engine use under medium-to-high load conditions, offering benefits like re-

duced soot and stable combustion. While ignition timing and emissions may require calibration, JP8 remains a viable alternative fuel. Although this study assessed JP8-diesel blends across various loads, further research is needed to optimize engine performance. Future work should explore advanced injection strategies (e.g., early, multiple, or split injections) and varied EGR rates to manage NO<sub>x</sub> emissions at high loads. Investigating low-temperature combustion modes like HCCI or RCCI could also help reduce both NO<sub>x</sub> and soot. Additionally, the long-term effects on injectors, fuel systems, and engine wear due to JP8's lower viscosity should be evaluated. Beyond steady-state conditions, future studies should examine cold start and transient operation performance. Finally, assessing compatibility with after-treatment systems (DPF, SCR) and testing a wider range of blend ratios or additives could further improve combustion quality and emissions, supporting broader military and civilian applications. While this study focused on energy-based performance and emission parameters, future research should also include exergy-based analyses to assess the second-law efficiency of JP8–diesel combustion. Such analyses could quantify irreversibilities, identify major sources of exergy destruction, and help optimize injection strategies or combustion phasing for maximum thermodynamic efficiency.

## Research Ethics

Not applicable.

## Artificial Intelligence Use

The author(s) state that generative AI tools (e.g., ChatGPT) were used only for language editing during manuscript preparation. No AI-generated content was used for analysis or interpretation. The authors take full responsibility for the integrity and accuracy of the content.

## Author Contributions

The author(s) have (has) accepted responsibility for the entire content of this manuscript and approved its submission.

Conceptualization: [Fazıl Akgün, Samet Çelebi, Usame Demir], Data curation: [Fazıl Akgün, Samet Çelebi], Formal analysis: [Fazıl Akgün, Samet Çelebi, Usame Demir], Investigation: [Fazıl Akgün, Samet Çelebi], Methodology: [Fazıl Akgün, Samet Çelebi, Usame Demir], Project administration: [Samet Çelebi], Resources: [Fazıl Akgün, Usame Demir], Supervision: [Samet Çelebi], Validation: [Fazıl Akgün, Samet Çelebi, Usame Demir], Visualization: [Fazıl Akgün, Usame Demir], Writing – original draft: Fazıl Akgün, Samet Çelebi], Writing – review & editing: [Fazıl Akgün, Samet Çelebi, Usame Demir]

## Competing Interests

The author(s) state(s) no conflict of interest.

## Research Funding

None declared.

## Data Availability

The raw data can be obtained on request from the corresponding author.

## Peer-review

Peer-reviewed by external referees.

## Orcid

Fazıl Akgün  <https://orcid.org/0000-0003-0087-6953>

Samet Çelebi  <https://orcid.org/0000-0002-4616-3935>

Usame Demir  <https://orcid.org/0000-0001-7383-1428>

## References

- [1] Park, Y., Bae, C., Mounaim-Rousselle, C., & Foucher, F. (2015). Application of jet propellant-8 to premixed charge ignition combustion in a single-cylinder diesel engine. *International Journal of Engine Research*, 16(1), 92–103. <https://doi.org/10.1177/1468087414561275>
- [2] Maurice, L. Q., Lander, H., Edwards, T., & Harrison, W. E. (2001). Advanced aviation fuels: A look ahead via a historical perspective. *Fuel*, 80(6), 747–756. [https://doi.org/10.1016/S0016-2361\(00\)00142-3](https://doi.org/10.1016/S0016-2361(00)00142-3)
- [3] Liu, Y., Sun, H., Wang, L., & Gao, Q. Y. (2025). ReaxFF MD investigation of different JP8 surrogates on combustion mechanism and reaction kinetics. *Canadian Journal of Chemical Engineering*. Advance online publication. <https://doi.org/10.1002/cjce.25647>
- [4] Yang, S., Moon, H., & Lee, C. (2017). A study of spill control characteristics of JP-8 and conventional diesel fuel with a common rail direct injection system. *Energies*, 10(12), 2104. <https://doi.org/10.3390/en10122104>
- [5] Pleil, J. D., Smith, L. B., & Zelnick, S. D. (2000). Personal exposure to JP-8 jet fuel vapors and exhaust at air force bases. *Environmental Health Perspectives*, 108(2), 183–192. <https://doi.org/10.1289/ehp.00108183>
- [6] Alabaş, B., Taştan, M., Özcan, A., & Amez, I. (2025). Flame characteristics and emission behaviors of JP8/biogas mixtures under external acoustic enforcement frequencies. *Fuel*, 388, 134516. <https://doi.org/10.1016/j.fuel.2025.134516>
- [7] Copulos, M. R. (2003). America's Achilles heel: The hidden costs of imported oil (pp. 40–53). National Defense Council Foundation.
- [8] Belcher, O., Bigger, P., Neimark, B., & Kennelly, C. (2020). Hidden carbon costs of the "everywhere war": Logistics, geopolitical ecology, and the carbon boot-print of the US military. *Transactions of the Institute of British Geographers*, 45(1), 65–80. <https://doi.org/10.1111/tran.12319>
- [9] Ryczyński, J., & Tubis, A. A. (2021). Tactical risk assessment method for resilient fuel supply chains for a military peacekeeping operation. *Energies*, 14(14), 4679. <https://doi.org/10.3390/en14154679>
- [10] Violi, A., Yan, S., Eddings, E. G., Sarofim, A. F., Granata, S., Faravelli, T., et al. (2002). Experimental formulation and kinetic model for JP-8 surrogate mixtures. *Combustion Science and Technology*, 174(5–6), 399–417. <https://doi.org/10.1080/00102200215080>
- [11] Liu, Y., Sun, H., Wang, L., & Gao, Q. Y. (2025). ReaxFF MD investigation of different JP8 surrogates on combustion mechanism and reaction kinetics. *Canadian Journal of Chemical Engineering*. Advance online publication. <https://doi.org/10.1002/cjce.25647>
- [12] Yamık, H., Calam, A., Solmaz, H., & İçingür, Y. (2014). Havacılık yakıtı JP-8 ve dizel karışımlarının tek silindirli bir dizel motorunda performans ve egzoz emisyonlarına etkisi. *Gazi Üniversitesi Mühendislik Mimarlık Fakültesi Dergisi*, 28, (Sayfa numarası belirtilmemiş).
- [13] Labeckas, G., Slavinskas, S., & Vilutienė, V. (2015). The effect of aviation fuel JP-8 and diesel fuel blends on engine performance and exhaust emissions. *Journal of KONES*, 22(2), 129–138. <https://doi.org/10.5604/12314005.1165418>
- [14] Ardebili, S. M. S., Kocakulak, T., Aytav, E., & Calam, A. (2022). Investigation of the effect of JP-8 fuel and biodiesel fuel mixture on engine performance and emissions by experimental and statistical methods. *Energy*, 254, 124155. <https://doi.org/10.1016/j.energy.2022.124155>
- [15] Fernandes, G., Fuschetto, J., Filipi, Z., Assanis, D., & McKee, H. (2007). Impact of military JP-8 fuel on heavy-duty diesel engine performance and emissions. *Proceedings of the Institution of Mechanical Engineers, Part D: Journal of Automobile Engineering*, 221(7), 957–970. <https://doi.org/10.1243/09544070JAUTO211>
- [16] Henein, N., Bryzik, W., Jayakumar, C., Sattler, E. R., Johnson, N. C., & Hubble, N. K. (2011). Autoignition characteristics of low cetane number JP-8 and approaches for improved operation in military diesel engines. <https://doi.org/10.4271/2024-01-3292>
- [17] Labeckas, G., Slavinskas, S., & Vilutienė, V. (2014). Effect of the cetane number improving additive on combustion, performance, and emissions of a DI diesel engine operating on JP-8 fuel. *Journal of Energy Engineering*, 141(2), C4014005. [https://doi.org/10.1061/\(ASCE\)EY.1943-7897.0000222](https://doi.org/10.1061/(ASCE)EY.1943-7897.0000222)
- [18] Dülger, Z., Aslan, S., Arici, M., Catori, C., Karabay, H., Polat, N., et al. (2014). Performance and emissions of a micro-turbine fueled with JP8-canola biodiesel mixtures. *Proceedings of the ASME Turbo Expo*, 1B. <https://doi.org/10.1115/GT2014-27340>
- [19] Fernandes, G., Fuschetto, J., Filipi, Z., Assanis, D., & McKee, H. (2007). Impact of military JP-8 fuel on heavy-duty diesel engine performance and emissions. *Proceedings of the Institution of Mechanical Engineers, Part D: Journal of Automobile Engineering*, 221(7), 957–970. <https://doi.org/10.1243/09544070JAUTO211>
- [20] Frame, E. A., & Blanks, M. G. (2004). Emissions from a 6.5 L HMMWV engine on low sulfur diesel fuel and JP-8. *US Army TARDEC Interim Report TFLRF*.
- [21] Kouremenos, D. A., Rakopoulos, C. D., & Hountalas, D. T. (1997). Experimental investigation of the performance and exhaust emissions of a swirl chamber diesel engine using JP-8 aviation fuel. *International Journal of Energy Research*, 21(12), 1173–1185.
- [22] Labeckas, G., & Slavinskas, S. (2021). Comparative evaluation of the combustion process and emissions of a diesel engine operating on the cetane improver 2-ethylhexyl nitrate doped rapeseed oil and aviation JP-8 fuel. *Energy Conversion and Management*, 211, 100106. <https://doi.org/10.1016/j.encon.2021.100106>
- [23] Fernandes, G., Fuschetto, J., Filipi, Z., Assanis, D., & McKee, H. (2007). Impact of military JP-8 fuel on heavy-duty diesel engine performance and emissions. *Proceedings of the Institution of Mechanical Engineers, Part D: Journal of Automobile Engineering*, 221(7), 957–970. <https://doi.org/10.1243/09544070JAUTO211>
- [24] Corporan, E., DeWitt, M. J., Klingshirm, C. D., Striebig, R., & Cheng, M. D. (2012). Emissions characteristics of military helicopter engines with JP-8 and Fischer-Tropsch fuels. *Journal of Propulsion and Power*, 26(2), 317–324. <https://doi.org/10.2514/1.43928>
- [25] Fernandes, G., Fuschetto, J., Filipi, Z., Assanis, D., & McKee, H. (2007). Impact of military JP-8 fuel on heavy-duty diesel engine performance and emissions. *Proceedings of the Institution of Mechanical Engineers, Part D: Journal of Automobile Engineering*, 221(7), 957–970. <https://doi.org/10.1243/09544070JAUTO211>
- [26] Likos, W. E., Owens, E. C., & Lestz, S. J. (1988). Laboratory evaluation of MIL-T-83133 JP-8 fuel in army diesel engines: Interim report, October 1984–January 1988. Southwest Research Institute.

- [27] Luning Prak, D., Fohner, D., Neubauer, J., Dickerson, T., Cowart, J., & Baker, B. (2023). The impact of navy jet fuel (JP-5) and diesel fuel (F-76) on the swelling and tensile strength of additivity-manufactured and commercially-manufactured O-rings. *Fuel*, 354, 129291. <https://doi.org/10.1016/j.fuel.2023.129291>
- [28] Uyumaz, A., Solmaz, H., Yilmaz, E., Yamik, H., & Polat, S. (2014). Experimental examination of the effects of military aviation fuel JP-8 and biodiesel fuel blends on the engine performance, exhaust emissions and combustion in a direct injection engine. *Fuel Processing Technology*, 128, 158–165. <https://doi.org/10.1016/j.fuproc.2014.07.013>
- [29] Tsanaksidis, C. G., Favvas, E. P., Tzilantonis, G. T., & Scaltsoyiannes, A. V. (2014). A new fuel (D–BD–J) from the blending of conventional diesel, biodiesel and JP8. *Fuel Processing Technology*, 127, 66–71. <https://doi.org/10.1016/j.fuproc.2014.06.003>
- [30] Tiktas, A., Gunerhan, H., & Hepbasli, A. (2024). Exergoeconomic optimization of a proposed novel combined solar powered electricity and high-capacity cooling load production system for economical and potent generation via utilization of low-grade waste heat source. *Thermal Science and Engineering Progress*, 55, 102976. <https://doi.org/10.1016/j.tsep.2024.102976>
- [31] Tiktas, A., Gunerhan, H., Hepbasli, A., & Açikkalp, E. (2024). Extended exergy analysis of a novel integrated absorptional cooling system design without utilization of generator for economical and robust provision of higher cooling demands. *Energy Conversion and Management*, 307, 118350. <https://doi.org/10.1016/j.enconman.2024.118350>
- [32] Özer, S., Tunçer, E., Demir, U., Gülcan, H. E., & Çelebi, S. (2025). Energy, exergy, exergoenvironmental, and exergoenvironmental assessment of a two stroke UAV small engine using JP5 aviation fuel and hydroxy (HHO) gas. *International Journal of Hydrogen Energy*, 143, 846–861. <https://doi.org/10.1016/j.ijhydene.2024.10.394>
- [33] Özer, S., Gülcan, H. E., Çelebi, S., & Demir, U. (2025). Assessment of waste tyre pyrolysis oil and oxy-hydrogen gas usage in a diesel engine in terms of energy, exergy, environmental, and enviroeconomic perspectives. *International Journal of Hydrogen Energy*, 143, 862–881. <https://doi.org/10.1016/j.ijhydene.2024.11.107>
- [34] Özer, S., Tunçer, E., Demir, U., & Gülcan, H. E. (2025). Thermodynamic, thermoeconomic, and exergoeconomic analysis of a UAV two stroke engine fueled with gasoline-octanol and gasoline-hexanol blends. *Energy Conversion and Management*, 327, 119545. <https://doi.org/10.1016/j.enconman.2025.119545>
- [35] Demir, U., Gülcan, H. E., & Özer, S. (2025). The effect of TiO<sub>2</sub> nano-additive on emissions, exergetic performance, and enviro/social/economic indicators in a small UAV jet engine fuelled with kerosene. *Fuel*, 390, 134725. <https://doi.org/10.1016/j.fuel.2025.134725>
- [36] Lutz, T., & Modiyani, R. (2011). Brake thermal efficiency improvements of a commercially based diesel engine modified for operation on JP 8 fuel. SAE 2011 World Congress and Exhibition. <https://doi.org/10.4271/2011-01-0120>
- [37] Sinha, A., & Sharma, A. (2020). Combustion analysis and simulation of JP-8 fuel in 4 stroke CI engine. *International Journal of Pollution and Noise Control*, 6(2), 21–28. <https://doi.org/10.37628/ijpn-v6i2.1159>
- [38] Gülcan, H. E., Gültekin, N., & Ciniviz, M. (2023). Effect of diesel injection pressure for enhancing combustion and reducing mechanical vibration and noise emissions in a non-road diesel engine. *European Mechanical Science*, 7(2), 199–208. <https://doi.org/10.26701/EMS.1337141>
- [39] Özer, S., Tunçer, E., Demir, U., Gülcan, H. E., & Çelebi, S. (2024). Energy, exergy, exergoenvironmental, and exergoenvironmental assessment of a two stroke UAV small engine using JP5 aviation fuel and hydroxy (HHO) gas. *International Journal of Hydrogen Energy*. Advance online publication. <https://doi.org/10.1016/j.ijhydene.2024.10.394>
- [40] Reşitoğlu, İ. A., Yaşar, A., & Keskin, A. (2018). Exhaust emissions of diesel engine with CuNO<sub>3</sub> nano additive and butanol-diesel blends. *European Mechanical Science*, 2(3), 106–110. <https://doi.org/10.26701/EMS.384443>
- [41] Yucer, C. T., & Nacakli, Y. (2024). Effects of the partial use of diesel fuel with kerosene on the exergetic sustainability performance of a UAV jet engine in case of emergency. In *Proceedings of the 2024 conference* (pp. 131–136). [https://doi.org/10.1007/978-3-031-42041-2\\_18](https://doi.org/10.1007/978-3-031-42041-2_18)
- [42] Kılıçalp, M. İ., & Demir, U. (2025). Performance, emission, vibration and noise characteristics of gasoline-based fuel blends with JP-8, Jet A-1, and nitromethane mixtures in a single-cylinder gasoline engine. *Fuel*, 393, 135034. <https://doi.org/10.1016/j.fuel.2025.135034>
- [43] Park, J., & Sim, H. S. (2024). Ignition and combustion characteristics of alternative fuel under high-temperature and high-pressure conditions. *Journal of the Korean Society of Combustion*, 29(1), 11–18.
- [44] Cengiz, C., Ayyıldız, A., Karagöz, S., Coşkun, A., & Berk, S. (2019). Combustion visualization of partially premixed and non-premixed diesel fuel on single cylinder optical engine. *European Mechanical Science*, 3(1), 24–31. <https://doi.org/10.26701/EMS.385475>
- [45] Pandey, A. K., Nandgaonkar, M., Varghese, A., Sonawane, C., Kohil, R., & Warke, A. (2023). Comparison and evaluation of engine wear, engine performance, NO<sub>x</sub> reduction and nanoparticle emission by using gasoline, JP-8, karanja oil methyl ester biodiesel, and diesel in a military 720 kW, heavy-duty CIDI engine applying EGR with turbo charging. *SAE Technical Papers*. <https://doi.org/10.4271/2023-01-0318>
- [46] Kavuri, C., Tiry, M., Paz, J., & Kokjohn, S. L. (2017). Experimental and computational investigation of soot production from a premixed compression ignition engine using a load extension injection. *International Journal of Engine Research*, 18(5), 573–590. <https://doi.org/10.1177/1468087416650073>